

Parametrization and Molecular Dynamics Simulations of Nitrogen Oxyanions and Oxyacids for Applications in Atmospheric and Biomolecular Sciences

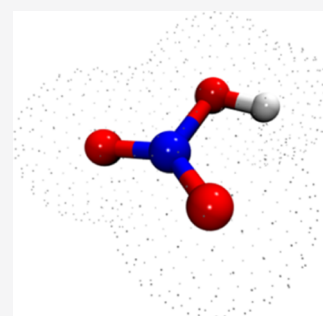
Rodrigo M. Cordeiro,* Maksudbek Yusupov, Jamoliddin Razzokov, and Annemie Bogaerts

 Cite This: *J. Phys. Chem. B* 2020, 124, 1082–1089 Read Online

ACCESS |

 Metrics & More Article Recommendations Supporting Information

ABSTRACT: Nitrogen oxyanions and oxyacids are important agents in atmospheric chemistry and medical biology. Although their chemical behavior in solution is relatively well understood, they may behave very differently at the water/air interface of atmospheric aerosols or at the membrane/water interface of cells. Here, we developed a fully classical model for molecular dynamics simulations of NO_3^- , NO_2^- , HNO_3 , and HNO_2 in the framework of the GROMOS 53A6 and 54A7 force field versions. The model successfully accounted for the poorly structured solvation shell and ion pairing tendency of NO_3^- . Accurate pure-liquid properties and hydration free energies were obtained for the oxyacids. Simulations at the water/air interface showed a local enrichment of HNO_3 and depletion of NO_3^- . The effect was discussed in light of earlier spectroscopic data and ab initio calculations, suggesting that HNO_3 behaves as a weaker acid at the surface of water. Our model will hopefully allow for efficient and accurate simulations of nitrogen oxyanions and oxyacids in solution and at microheterogeneous interface environments.



1. INTRODUCTION

Nitrate (NO_3^-) and nitrite (NO_2^-) are common nitrogen oxyanions that constitute the basic forms of nitric (HNO_3) and nitrous (HNO_2) acid. These species exist as natural or anthropogenic constituents of atmospheric aerosols and play an important role in climate, pollution, and public health issues.¹ In the food industry, they are largely employed as preservatives, with concerns being raised about their potential carcinogenic side-effects.² Under controlled conditions, however, they may turn out to be very useful in medical applications. For instance, photodynamic therapy³ and plasma-based cancer treatments⁴ rely on the delivery of reactive oxygen and nitrogen species (RONS) to the tumoral tissue, culminating in localized cell death.

Whether in the atmosphere or in the organism, chemical and physical processes are influenced by interfaces. The water/air interface of atmospheric aerosols and the membrane/water interface of cells are environments where chemical reactions take place, including those involving nitrogen oxyanions and oxyacids. To understand these processes, it is helpful to have molecular models and computer simulation tools that are efficient and accurate, especially at microheterogeneous interface environments. However, even the description of bulk-phase solvation can be challenging. Neutron diffraction measurements^{5,6} and ab initio calculations^{7–10} have consistently revealed a poorly structured hydration shell around NO_3^- , while classical molecular-mechanics models tended to overestimate ion–solvent¹⁰ and even ion–ion¹¹ interactions. It has been noted that the rigid structure of typical water models and the use of atomic point charges may produce coordination

shells that are artificially well structured.⁶ This issue becomes critical in the case of NO_3^- and NO_2^- because of charge delocalization, from which one would rather expect smoother charge distributions and stronger polarizability. In principle, these effects could be incorporated into a classical model by distributing the ionic charge into additional virtual sites or by adding a polarization term to the force field. However, each of these improvements has its drawbacks with regards to computational efficiency and stability.¹²

To the best of our knowledge, there is no molecular-mechanical model in the literature for nitrogen oxyanions that also comprises their conjugated acid forms. With a pK_a of -1.38 ,¹³ HNO_3 is one of the strongest inorganic acids, found in water almost exclusively in the ionized form. However, spectroscopic measurements¹⁴ and ab initio calculations^{15–18} have shown that the molecular form of HNO_3 is stabilized at the water/air interface, meaning that HNO_3 behaves as a weaker acid in this region. It is true that fully classical models do not incorporate the electronic degrees of freedom that are necessary to explicitly describe protonation/deprotonation events. However, local changes in the acid ionization constant (K_a) are closely related to the partitioning of the involved species between the aqueous bulk and the interface region, as

Received: August 27, 2019

Revised: January 2, 2020

Published: January 21, 2020

Parametrization and Molecular Dynamics Simulations of Nitrogen Oxyanions and Oxyacids for Applications in Atmospheric and Biomolecular Sciences

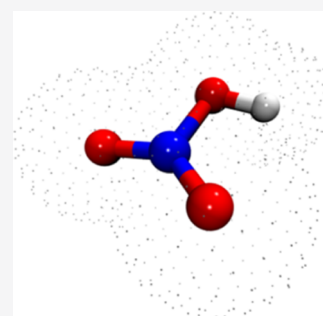
Rodrigo M. Cordeiro,* Maksudbek Yusupov, Jamoliddin Razzokov, and Annemie Bogaerts

 Cite This: *J. Phys. Chem. B* 2020, 124, 1082–1089 Read Online

ACCESS |

 Metrics & More Article Recommendations Supporting Information

ABSTRACT: Nitrogen oxyanions and oxyacids are important agents in atmospheric chemistry and medical biology. Although their chemical behavior in solution is relatively well understood, they may behave very differently at the water/air interface of atmospheric aerosols or at the membrane/water interface of cells. Here, we developed a fully classical model for molecular dynamics simulations of NO_3^- , NO_2^- , HNO_3 , and HNO_2 in the framework of the GROMOS 53A6 and 54A7 force field versions. The model successfully accounted for the poorly structured solvation shell and ion pairing tendency of NO_3^- . Accurate pure-liquid properties and hydration free energies were obtained for the oxyacids. Simulations at the water/air interface showed a local enrichment of HNO_3 and depletion of NO_3^- . The effect was discussed in light of earlier spectroscopic data and ab initio calculations, suggesting that HNO_3 behaves as a weaker acid at the surface of water. Our model will hopefully allow for efficient and accurate simulations of nitrogen oxyanions and oxyacids in solution and at microheterogeneous interface environments.



1. INTRODUCTION

Nitrate (NO_3^-) and nitrite (NO_2^-) are common nitrogen oxyanions that constitute the basic forms of nitric (HNO_3) and nitrous (HNO_2) acid. These species exist as natural or anthropogenic constituents of atmospheric aerosols and play an important role in climate, pollution, and public health issues.¹ In the food industry, they are largely employed as preservatives, with concerns being raised about their potential carcinogenic side-effects.² Under controlled conditions, however, they may turn out to be very useful in medical applications. For instance, photodynamic therapy³ and plasma-based cancer treatments⁴ rely on the delivery of reactive oxygen and nitrogen species (RONS) to the tumoral tissue, culminating in localized cell death.

Whether in the atmosphere or in the organism, chemical and physical processes are influenced by interfaces. The water/air interface of atmospheric aerosols and the membrane/water interface of cells are environments where chemical reactions take place, including those involving nitrogen oxyanions and oxyacids. To understand these processes, it is helpful to have molecular models and computer simulation tools that are efficient and accurate, especially at microheterogeneous interface environments. However, even the description of bulk-phase solvation can be challenging. Neutron diffraction measurements^{5,6} and ab initio calculations^{7–10} have consistently revealed a poorly structured hydration shell around NO_3^- , while classical molecular-mechanics models tended to overestimate ion–solvent¹⁰ and even ion–ion¹¹ interactions. It has been noted that the rigid structure of typical water models and the use of atomic point charges may produce coordination

shells that are artificially well structured.⁶ This issue becomes critical in the case of NO_3^- and NO_2^- because of charge delocalization, from which one would rather expect smoother charge distributions and stronger polarizability. In principle, these effects could be incorporated into a classical model by distributing the ionic charge into additional virtual sites or by adding a polarization term to the force field. However, each of these improvements has its drawbacks with regards to computational efficiency and stability.¹²

To the best of our knowledge, there is no molecular-mechanical model in the literature for nitrogen oxyanions that also comprises their conjugated acid forms. With a pK_a of -1.38 ,¹³ HNO_3 is one of the strongest inorganic acids, found in water almost exclusively in the ionized form. However, spectroscopic measurements¹⁴ and ab initio calculations^{15–18} have shown that the molecular form of HNO_3 is stabilized at the water/air interface, meaning that HNO_3 behaves as a weaker acid in this region. It is true that fully classical models do not incorporate the electronic degrees of freedom that are necessary to explicitly describe protonation/deprotonation events. However, local changes in the acid ionization constant (K_a) are closely related to the partitioning of the involved species between the aqueous bulk and the interface region, as

Received: August 27, 2019

Revised: January 2, 2020

Published: January 21, 2020

conceptually demonstrated by the thermodynamic cycle in Figure 1a. Assuming that the pH does not change from the

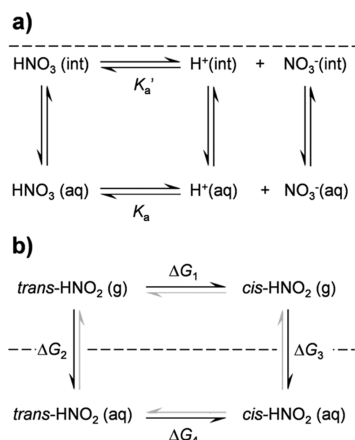


Figure 1. (a) Thermodynamic cycle relating local changes in the ionization constant (K_a) of HNO₃ with the partitioning of the involved species between the aqueous bulk (aq) and the water/air interface (int, dashed line). (b) Thermodynamic cycle relating the hydration of HNO₂ conformers and isomerization at the gas (g) and aqueous phases. Free energy variations ΔG_i refer to processes occurring in the direction of the darker arrows.

bulk to the interface, an interface-induced drop in K_a should translate into the interfacial enrichment of HNO₃ and depletion of NO₃[−]. In principle, a successful molecular mechanical model should capture this tendency at least on the qualitative level.

With that in mind, we present the systematical development of a GROMOS-type¹⁹ molecular-mechanical model for NO₃[−], NO₂[−], HNO₃, and HNO₂. We validated the model by showing that it successfully accounted for solvation properties and ion-pairing tendencies of these species. Most importantly, the model captured experimentally supported interfacial phenomena, such as the enrichment of HNO₃ at the water surface¹⁴ and the surface-induced ion-pairing of NaNO₂.²⁰ Many well-established force field families are framed within the rules of simplicity (i.e., functional form with as few terms as possible), versatility (i.e., modularity and transferability of molecular building blocks), and efficiency (i.e., computational speed). Our molecular model was developed with the same philosophy and thus represents a useful tool for large-scale simulations of various kinds of interfacial environments in chemistry and biology.

2. COMPUTATIONAL METHODS

2.1. General Setup and Parametrization Philosophy.

Molecular dynamics (MD) simulations²¹ were performed with GROMACS 5.0.4.^{22,23} Newton's equations of motion were solved with the following setup: time step of 2 fs; bond length constraints; periodic boundary conditions; particle mesh Ewald (PME) electrostatics with a real-space cutoff of 0.9 nm; double-range truncation of Lennard-Jones interactions at 0.9 and 1.4 nm; and long-range dispersion corrections of energy and pressure. Interatomic interactions were based on the framework of the GROMOS 53A6 force field and the SPC water model.¹⁹ The parametrization of nitrogen oxyanions and oxyacids followed a trial-and-error approach, in which force field parameters were iteratively adjusted to match reference data from more fundamental ab initio calculations and

experiments. Force field and molecular topology files are available as [Supporting Information](#). Force field data are also summarized in [Table S1](#).

2.2. Parametrization of Nitrogen Oxyanions. The molecular geometries of NO₃[−] and NO₂[−] were taken from earlier molten salt parametrizations.^{24,25} Lennard-Jones interactions were selected from the existing GROMOS database and partial atomic charges were adjusted for a correct description of the hydration structure and ion pairing in solution. Various systems were simulated, ranging from the infinitely dilute regime (i.e., a single ion pair in a 3 × 3 × 3 nm³ water box), up to a concentration of ~4.5 mol/L. Equilibration took place at the isothermal–isobaric (NPT) ensemble at 1 bar and 298 K for 5 ns, followed by data acquisition for 25 ns. Radial and spatial distribution functions (RDF and SDF, respectively) were computed to show the distribution of hydration waters and Na⁺ counter ions around NO₃[−] and NO₂[−]. The positions of the minima after the first RDF peaks were used as distance cutoffs for the determination of hydration numbers and ionic pairs. Diffusion coefficients were calculated from the mean square displacement of the anions.

2.3. Parametrization of Nitrogen Oxyacids. We relied on earlier ab initio calculations and spectroscopic data to describe the internal structure and conformational equilibrium of nitrogen oxyacids.^{26–31} The HNO₃ model was assembled based on small adaptations to the Lennard-Jones parameters previously developed for small and electrically neutral RONS.^{32,33} Atom-centered partial charges were initially estimated from electronic structure calculations using Gaussian 09.³⁴ B3LYP density functional calculations were performed with the 6-311++G(3df,3pd) basis set, followed by CHelpG fitting of the electrostatic potential. Partial charges were then iteratively scaled up in order to account for polarization effects at the condensed phase, and provide an optimized description of pure-liquid and hydration properties. Pure HNO₃ was equilibrated for 5 ns and sampled for the same duration for computation of its density and heat of vaporization.^{19,32} The hydration free energy at infinite dilution (ΔG_{hyd}) of HNO₃ was calculated via the thermodynamic integration (TI) method.²¹ A single HNO₃ molecule was placed in a 3 × 3 × 3 nm³ water box and TI was performed at 1 bar and 298 K. Each TI calculation was partitioned into 72 individual simulation runs describing distinct solute–solvent coupling states, which were combined to yield ΔG_{hyd} (c.f. [eq S1](#)). At each intermediate state, the system was equilibrated for 600 ps and sampled for 5 ns. Further details are provided as [Supporting Information](#).

Parametrization of HNO₂ followed a similar route. However, additional considerations were needed because of the existence of two stable conformational states, *cis*- and *trans*-HNO₂. These states contribute together to the experimentally measured ΔG_{hyd} of HNO₂, but are separated by a large energy barrier.^{29–31} A complete exploration of the conformational space would require prohibitively long TI simulations. Enhanced sampling methods such as metadynamics have been successful in dealing with similar situations.³⁵ Here, however, we chose to pursue a simpler, yet thermodynamically equivalent approach. First, we assembled one set of force field parameters to describe both *cis*- and *trans*-HNO₂ ([Table S1](#)). CHelpG charges obtained for each conformer were averaged out and employed as starting values for the iterative charge optimization. We did not employ any particular optimization algorithm. Instead, charges were gradually scaled up by

successive trials aiming at a ΔG_{hyd} value within ~ 1 kJ/mol of reference data. Next, we set up a thermodynamic cycle to relate the conformational equilibria of HNO_2 in the gas and aqueous phases, as depicted in Figure 1b. We considered the weighted contributions of both conformers to the overall Henry's law constant of HNO_2 (eqs S2 to S4), resulting in the following expression for the overall hydration free energy (ΔG) of HNO_2

$$\Delta G = \Delta G_2 - RT \ln \frac{1 + \exp(-\Delta G_4/RT)}{1 + \exp(-\Delta G_1/RT)} \quad (1)$$

where R is the ideal gas constant, T is the temperature, and $\Delta G_4 = \Delta G_1 - \Delta G_2 + \Delta G_3$ is calculated according to the thermodynamic cycle in Figure 1b. The ΔG_1 term was derived directly from the torsional potential employed in the topological description of HNO_2 . Finally, ΔG_2 and ΔG_3 were determined by TI. Given that isomerization was extremely unlikely within 5 ns simulation windows, TI could be performed for each conformer separately. In less than 1% of the individual TI windows, isomerization occurred and simulations had to be reinitiated to ensure sampling of only the desired conformational state.

2.4. Simulations at the Water/Air Interface. A water slab with a $5.6 \times 5.6 \text{ nm}^2$ surface area and a thickness of ~ 5.6 nm was assembled with 5500 molecules. In total, 20 units of each of the following species were added together: NO_3^- , NO_2^- , HNO_3 , HNO_2 (initially trans), and HNO_2 (initially cis). Individual concentrations were equivalent to ~ 0.2 mol/L. A total of 40 Na^+ counter ions were added to keep electroneutrality. Equilibration was run at 310 K for 100 ns to allow enough time for HNO_2 isomerization, followed by 50 ns of sampling to determine the distribution and spatial configurations of the different species as a function of position across the water/air interface. A shorter simulation was performed with only ions, but at a 10-fold higher concentration. In this case, equilibration was performed for 30 ns, followed by sampling for 35 ns. The tendency for ion pairing was quantified as a function of the distance to the water/air interface.

3. RESULTS AND DISCUSSION

3.1. Hydration Structure of Nitrogen Oxyanions. It is well known that NO_3^- has a poorly structured hydration shell.^{5–10} Therefore, the NO_3^- model was assembled with the relatively large atom types “NR” and “OM”, whose Lennard-Jones interactions are described by large repulsive terms. In the GROMOS force field, Lennard-Jones interactions are defined in terms of atom types, with “OM” being the standard atom of choice for the description of anionic carboxylate groups. Atom-centered point charges of $+0.65e$ and $-0.55e$ were considered for nitrogen and oxygen, respectively. As depicted in Figure 2, the hydration structure of our NO_3^- model was in reasonable agreement with ab initio MD data and showed a significant improvement over earlier fully classical MD models.¹⁰ The ion–water RDFs exhibited little structuring, suggesting that water molecules were only weakly H-bonded to NO_3^- . SDFs revealed that coordinating waters were preferably located at the equatorial O–N–O bisector regions, in agreement with ab initio data.⁸ We speculate that the spatially anisotropic hydration structure of NO_3^- might play a role in its interactions and reactivity, in the sense that the out-of-plane

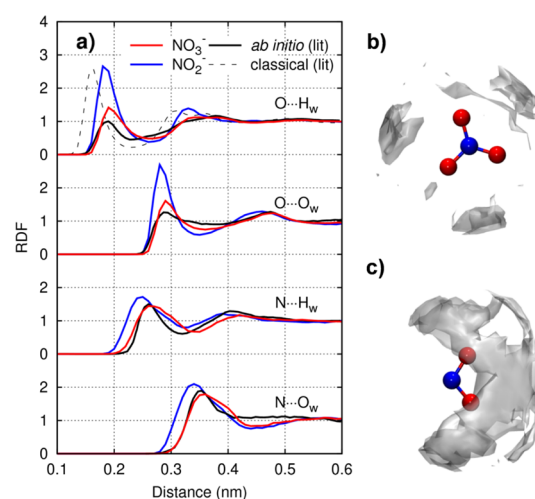


Figure 2. Hydration structure of nitrogen oxyanions at infinite dilution. (a) Ion–water radial distribution functions for NO_3^- (red) and NO_2^- (blue), as obtained from our MD simulations. Results are compared to ab initio (black) and classical (dashed) simulations of NO_3^- from the literature (lit).¹⁰ Three-dimensional spatial distribution of hydrating waters around (b) NO_3^- and (c) NO_2^- . The grey surfaces enclose regions where the local water density was at least 2.5 times higher than in the bulk.

regions of NO_3^- are less hydrated and therefore free to interact with other molecules.

The NO_2^- model was assembled with the same atom types as NO_3^- , but with partial charges of $+0.4e$ and $-0.7e$ for nitrogen and oxygen, respectively. It is also shown in Figure 2 that NO_2^- had a more structured hydration shell than NO_3^- . H-bonds were established mainly between its oxygen atoms and water, with fewer solvent molecules coordinated to the nitrogen atom. This is in qualitative agreement with ab initio quantum mechanical charge field MD results,³⁶ which were taken as reference for NO_2^- parametrization. We emphasize that the partial charges of the ions were empirically adjusted by trial-and-error and that their values played a critical role in the hydration structure of NO_2^- . Point charges directly derived from electronic structure calculations in a vacuum (B3LYP/6-311++G(3df,3pd)/CHelpG) were not as effective in reproducing the preference of water for the oxygen sites of NO_2^- (Figure S1). Continuum solvent quantum mechanical models or empirical corrections need to be employed to account for solvent-induced polarization. Our empirical charge set implicitly incorporates solvent-induced polarization effects that are necessary for the proper description of NO_2^- hydration. As a side note, CHelpG charges performed worse in NO_2^- than in NO_3^- , where H-bonding appeared to be less important. However, even in the case of NO_3^- , we opted to employ an empirical charge set with lower absolute values than the CHelpG charges. Our empirical charge set emphasized charge delocalization in NO_3^- and led to less structured coordination shells. The importance of this result lies in the fact that models based on point-charges and rigid solvent tend to produce excessively structured hydration shells.⁶

The properties obtained for NO_3^- and NO_2^- solutions are summarized in Table 1 and compared to reference experimental data. A total of 7–8 coordinating waters were found around both NO_3^- and NO_2^- , irrespective of concentration. These values were consistently higher than the experimental data of Kameda et al.,^{5,37} but we note that the

Table 1. Properties of Nitrogen Oxyanions and Oxyacids^a

compound	concentration ^b	ρ (kg/m ³)	ΔH_{vap} (kJ/mol)	ΔG_{hyd} (kJ/mol)	n_{hyd}	D (10 ⁻⁹ m ² /s)	refs
NO ₃ ⁻	dil				7.5	3.0 [1.902]	40
	1 mol/L				7.5		
	4.4 mol/L	1199 [1206]			7.4 [5.0]		5,39
NO ₂ ⁻	dil				7.1	2.7 [1.912]	40
	4.7 mol/L	1219 [1209]			6.7 [3.7]		37,39
HNO ₃	pure	1390 [1504]	41.0 [39.1]				40,46
	dil			-37.8 [-38]			47,48
<i>trans</i> -HNO ₂	dil			-18.0			
<i>cis</i> -HNO ₂	dil			-11.2			
HNO ₂	dil			-17.1 ^c [-17.6]			47,48

^aDensity (ρ), heat of vaporization (ΔH_{vap}), hydration free energy (ΔG_{hyd}), hydration number (n_{hyd}) and diffusion coefficient (D). Simulation results are presented along with reference experimental data within brackets. Uncertainties in the last digits. ^bThe entry dil stays for “infinitely dilute”. ^cWeighted average between conformers, according to eq 1.

hydration numbers reported for NO₃⁻ vary widely in the literature.³⁸ Our results closely agreed with the number of 8 coordinating waters found in recent ab initio MD simulations.^{9,10} The diffusion coefficients from simulations were also consistently higher than experimental reference data, but in the same order of magnitude. Within uncertainty, diffusion coefficients were practically the same for NO₃⁻ and NO₂⁻, much in line with experimental data. Even though NO₃⁻ is bigger than NO₂⁻, the latter has a larger hydrodynamic radius, that is, it drags a larger number of water molecules as it diffuses. This effect, which is also corroborated by the RDFs in Figure 2, has been used as an explanation for the fact that aqueous solutions of NO₂⁻ tend to be more viscous than analogous NO₃⁻ solutions over a large concentration and temperature range.³⁹

3.2. Ion Pairing in Aqueous Solution. Nitrates and nitrites are characterized by very high aqueous solubilities that may well exceed 10 mol in 1 L of water.⁴⁰ Using our newly developed model for NO₃⁻ and NO₂⁻, we were able to simulate NaNO₃ and NaNO₂ aqueous solutions that remained stable at concentrations as high as ~4.5 mol/L. As summarized in Table 1, the densities of the concentrated solutions agreed very well with experimental reference data. Figure 3 shows a panorama of ionic interactions in concentrated solutions of NaNO₃ and NaNO₂. In both cases, the trajectories revealed a rapid sequence of ion pairing and separation events. Na⁺ ions paired mostly with only one anion, forming electrically neutral pairs. Less often, however, larger ionic clusters were formed. Ion pairs and larger clusters were short-lived, with lifetimes that did not exceed a few hundreds of picoseconds. The formation of ion pairs was reflected on the ion–ion RDFs by means of the first peak at distances below 0.4 nm. This peak was higher for NO₂⁻ than for NO₃⁻, which indicates a larger tendency for ion pairing in NO₂⁻. Simulations performed using a different set of CHelpG partial charges led to similar results (Figure S2).

The formation of ion pairs in aqueous solution is an important phenomenon that reflects the quality and balance of ionic interactions in the force field. Our results are in discrepancy with earlier semi-empirical quantum mechanical/molecular mechanical simulations, which indicated the existence of both stronger and longer-lived ion pairing in NaNO₃ and NaNO₂ aqueous solutions.⁴¹ Ion–ion RDFs obtained from recent MD simulations of alkali nitrates also showed higher peaks.¹¹ In that investigation, however, crystallization was witnessed at concentrations well below the

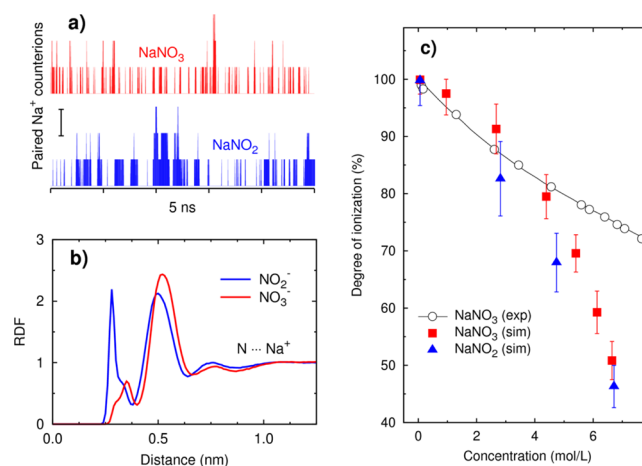


Figure 3. Ion pairing in aqueous solutions of nitrogen oxyanions. (a) 5 ns trajectory excerpts for selected NO₃⁻ and NO₂⁻ anions, showing the temporal fluctuations in the number of paired Na⁺ counterions. The vertical bar indicates the unity scale of the ordinate (i.e., one ion pair). (b) Ion–ion radial distribution functions at the high-concentration regime. (c) Degrees of ionization at several concentrations, as compared to experimental data from the literature for NaNO₃.⁴²

solubility limit. As shown in Figure 3c, the lower propensity for ion pairing in our model appears to be well aligned with experimental measurements.⁴² In the case of NaNO₃, ionization was almost complete at dilute solutions, but decreased to a ratio of ~80% at 4.4 mol/L, which is still within its solubility limit. Beyond 4.4 mol/L, the ion-pairing in the simulations was stronger as compared to the experimental data. Larger aggregates were formed, which might indicate the onset of nucleation. Further force field improvements could be achieved by considering not only the solution but also solid-state properties of NaNO₃. However, the “near-precipitation” thermodynamic state is beyond the scope of this work because a concentration of 4.4 mol/L already represents an excessively large ionic strength for most biomolecular simulations. The ionization degree of NaNO₂ was comparably lower than of NaNO₃ at similar concentrations. Currently, there is no reference experimental data on ionic interactions of NaNO₂. It would be interesting to test the predictions of our model as experimental data on NaNO₂ ion pairing become available.

Although our force field was developed based on GROMOS 53A6, it can be extended to later versions. The 54A7 version has been developed for an improved description of the protein

secondary structure.⁴³ All atom types, which define the Lennard-Jones interactions, were merely imported from the earlier 53A6 version. Combination of our model oxyanions with GROMOS 54A7 would seem straightforward, as the interactions with water and protein residues remain unaffected. However, Na^+ interactions have been reparametrized in GROMOS 54A7. If our oxyanion models are simply included in GROMOS 54A7 with no further changes, the description of ionic pairing improves for concentrations up to 1 mol/L. A slightly poorer description of ion pairing is obtained at the highest ionic strength (Figure S2), which is well beyond the conditions employed in most protein simulations.

3.3. Structure, Pure-Liquid Properties, and Hydration Energies of Nitrogen Oxyacids. The HNO_3 model was consistent with its well-known planar structure. Two symmetrically equivalent configurations of HNO_3 were possible as a result of the flipping of the O–N–O–H dihedral angle. They were equally stable, but separated by a large energy barrier of 32.8 kJ/mol.²⁷ The model was assembled with the atom types “NQ” and “OQ” at the $-\text{NO}_2$ fragment and “OP” and “H” at the $-\text{OH}$ fragment.^{32,33} The “OQ–OP” interaction was made more repulsive in order to improve the pure-liquid properties of the HNO_3 model. We emphasize that GROMOS interactions are individually defined for each pair type¹⁹ and that changes in the “OQ–OP” interaction bear no influence to the preceding parametrization work performed for RONS.^{32,33,44,45} The partial charges were then optimized, resulting in a HNO_3 model that yielded pure-liquid density and heat of vaporization values within $\pm 8\%$ of reference experimental data^{40,46} (c.f. Table 1). Solvation properties were in even closer agreement, with $\pm 1\%$ differences in ΔG_{hyd} between simulations and experiments.^{47,48} It should be realized that we employed PME electrostatics and long-range dispersion corrections in our simulation setup, which although not standard in GROMOS, may be preferred in particular situations, for instance in membrane simulations. Using exactly the same force field parameters, we repeated the calculations for HNO_3 employing the standard reaction field electrostatics without dispersion correction and found a variation of less than 3% in the properties of HNO_3 (data not shown).

The HNO_2 model successfully accounted for its gas-phase conformational behavior. *trans*- HNO_2 had the lowest energy and was separated from *cis*- HNO_2 by a small energy difference of 1.56 kJ/mol (corresponding to ΔG_1) and a large isomerization barrier of 39 kJ/mol.^{30,31} In aqueous solution, HNO_2 was mostly hydrated around its $-\text{OH}$ fragment, as shown in Figure 4a. Configurations around the energy minima were thoroughly explored within short 5 ns simulations, but full isomerization events were rare (Figure 4b). TI simulations were well-converged for individual conformers (Figure S3). As shown in Table 1, the aqueous environment increased the stability of *trans*- over *cis*- HNO_2 , with a free energy difference $\Delta G_4 = 8.4$ kJ/mol between the hydrated conformers. We explain this result by considering that the *trans* conformation leads to a larger molecular dipole moment. Following eq 1, the weighted average between both conformers led to an overall ΔG_{hyd} value in close agreement with experimental data for HNO_2 .

3.4. Nitrogen Oxyanions and Oxyacids at the Water/Air Interface. Figure 5 shows the distributions of NO_3^- , NO_2^- , HNO_3 , and HNO_2 across the water/air interface. The density of water molecules decreased smoothly from the bulk aqueous to the vapor phase, giving rise to a ~ 1 nm-thick

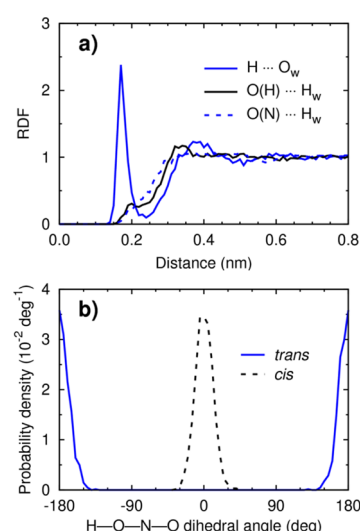


Figure 4. Hydration structure and conformational behavior of HNO_2 . (a) Radial distribution functions of hydrating waters around *trans*- HNO_2 . (b) Sampling of the conformational space by *cis*- and *trans*- HNO_2 during 5 ns simulations in aqueous solution.

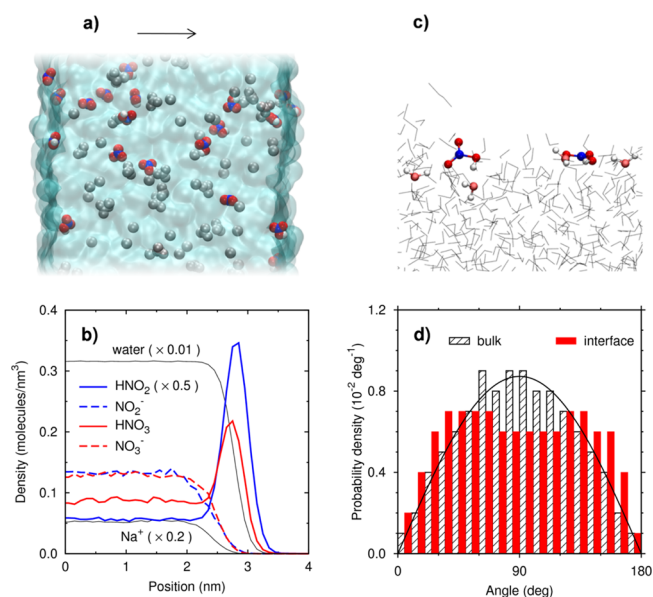


Figure 5. Interfacial behavior of nitrogen oxyanions and oxyacids. (a) Image of the equilibrated water slab (blue region), with NO_3^- and Na^+ represented as grey van der Waals spheres and HNO_3 highlighted in color (white H, red O, and blue N). The arrow points to the surface normal direction. (b) Local concentrations as a function of the distance from the slab center. Some distributions were scaled by the factors within brackets for better visualization. (c) Detailed image of two interfacial HNO_3 molecules with H-bonded hydration waters. (d) Local distributions of the relative angle between the normal vectors of the HNO_3 molecular plane and the interface plane. The black line represents a theoretical random distribution.

interfacial region. The NO_3^- and NO_2^- ions remained excluded from this region, in agreement with earlier MD simulations performed with a polarizable force field.^{49,50} On the other hand, the electrically neutral, acidic forms of HNO_3 and HNO_2 accumulated at the interface, reaching local concentrations many times larger than in the bulk aqueous phase. We did not draw a distinction between *cis*- and *trans*- HNO_2 because simulations were long enough to allow for a

significant number of isomerization events. Indeed, the *cis*/*trans* ratio evolved from 1:1 at the beginning of the simulation to 1:24 at equilibrium, in consistency with the ΔG_4 value (Figure S4). In the case of HNO_3 , both parallel and perpendicular orientations of the molecular plane were possible with respect to the surface, but the proportion of parallel arrangements was somewhat larger than expected for a completely random distribution.

The fact that HNO_3 accumulated at the interface, while its conjugated base NO_3^- was excluded from it, ultimately translates into HNO_3 being a weaker acid at the interface than in the bulk (c.f. Figure 1a). This conclusion follows directly from the definition of a position-dependent $\text{p}K_a$ shift, as

$$\Delta \text{p}K_a(z) = \Delta \text{pH}(z) - \log \frac{C_b(z)/C_b^\infty}{C_a(z)/C_a^\infty} \quad (2)$$

where z designates the position along the water/air interface and C the position-dependent concentrations of the acidic (a) and basic (b) forms at equilibrium (see also eqs S5 and S6). In classical simulations, the base/acid ratio in the bulk (C_b^∞/C_a^∞) is arbitrarily defined based on the initial number of molecules placed at the aqueous phase. However, note that eq 2 allows expressing $\Delta \text{p}K_a$ not as a function of absolute concentrations, but rather of ratios between local and bulk concentrations. With the distributions in Figure 5b and the rather crude assumption of no spatial pH variation, eq 2 predicts a $\text{p}K_a$ increase that can exceed one unit at the interface (Figure S5). However, given the qualitative nature of our analysis, this figure is probably best taken as a higher-bound estimate of $\Delta \text{p}K_a$. In fact, theoretical calculations have suggested that the auto-ionization of water may be slightly favored near the interface.⁵¹ That would have the effect of enhancing the local concentration of H_3O^+ ions, which would in turn lead to a lower $\Delta \text{p}K_a$ according to eq 2. The interfacial stabilization of HNO_3 in its molecular form is also supported by experimental data. X-ray photoelectron spectroscopy has revealed a $\sim 20\%$ decrease in HNO_3 ionization at the solution interface.¹⁴ This value is likely to be underestimated because one cannot easily distinguish between contributions of the top and subsurface layers. Indeed, our simulations suggest that the effect is confined to an interface layer narrower than 1 nm. That might explain why no change in HNO_3 ionization has been detected in a different investigation using glancing-angle Raman spectroscopy, with an estimated probing depth of 50–100 nm.⁵²

Another interesting spectroscopic observation is that NO_2^- ions are able to populate the water/air interface in the form of ion pairs.²⁰ Figure 6 shows the variations of the ionic pairing tendencies of NaNO_3 and NaNO_2 across the water/air interface, as recorded during simulations performed with ~ 2 mol/L of each salt. As seen earlier, ions were for the most part excluded from the interface. However, for the few ions that reached the surface, ion pairing was favored. The degree of ionization dropped at the outermost interface layers, where the hydration level was less than 10% as in the bulk. Any experimental technique designed to probe nitrogen oxyanions at the interface is likely to produce a response signal with a significant contribution from ion pairs. Interfacial properties, such as surface tension, are also likely to be affected by the increased prevalence of ion pairs relative to the dissociated ions at the surface.

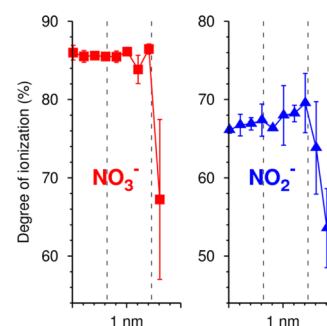


Figure 6. Ion pairing of nitrogen oxyanions within a 1 nm-thick region at the water/air interface of a concentrated solution. Vertical dashed lines indicate the region where the water density drops from 90 to 10% of its bulk value. Error bars were estimated based on the variation of the results among both surfaces of the water slab.

3.5. Applications in Atmospheric and Biomolecular Sciences.

Nitrogen oxyanions and oxyacids are well-known components of atmospheric aerosols.¹ Chemical speciation within aqueous aerosol particles may be largely influenced by the interface because of their large surface-to-volume ratios. Although nitrogen oxyanions and oxyacids were not explicitly interconvertible in our simple molecular-mechanical formalism, the model was still successful in reproducing the larger surface activity of the protonated species as compared to their anionic counterparts. That implies a surface-induced stabilization of the molecular forms of HNO_3 and HNO_2 over NO_3^- and NO_2^- , respectively. The implications for atmospheric chemistry are from the fact that interfacial reactions are likely to occur in a more acidic environment than expected from the bulk pH. It is true that *ab initio* MD simulations will continue to be the preferred method for studying the dynamics of chemical reactions. However, the time scales that can be achieved are still severely limited by current computational resources. A fully classical model of nitrogen oxyanions and oxyacids allows for a statistically more complete analysis of phenomena such as molecular diffusion, partitioning, and reorientation. A reliable and well-validated classical model can be used to generate interaction and hydration configurations of molecules at the air/water interface, later to be employed as starting points for more detailed *ab initio* calculations of chemical reactions.

The advantage of higher efficiency becomes more evident in the case of biomolecular simulations. Proteins, membranes, and other biological structures are often too large for a full quantum mechanical treatment. As an example of biological application, we can consider the interaction between cell membranes and plasma (i.e., ionized gas) species. Plasma-based skin treatments generate large quantities of NO_3^- and NO_2^- , which have been found to permeate all skin layers very effectively, including the stratum corneum.⁵³ To reconcile this observation with the low ionic permeability of phospholipid membranes, we speculate that nitrogen oxyanions may reside at the membrane surface and traverse its hydrophobic interior in their conjugated acid form. Further studies are underway to investigate this issue. We also point out that NO_3^- and NO_2^- are potential targets of enzymatic action.⁵⁴ Studies of enzyme-anion binding may profit from a well-balanced description of ionic interactions.

4. CONCLUSIONS

We developed a fully classical model for MD simulations of NO_3^- , NO_2^- , HNO_3 , and HNO_2 in the framework of the GROMOS 53A6 and 54A7 force field versions. The model successfully accounted for: (i) the poorly structured solvation shell of NO_3^- and the anisotropic water distribution around NO_2^- ; (ii) a well-balanced ion-pairing tendency in NaNO_3 solutions; (iii) accurate pure-liquid properties and hydration free energies of HNO_3 and HNO_2 ; (iv) the stabilization of the molecular form of HNO_3 at the water/air interface; and (v) the increased ion-pairing tendency of NaNO_2 at the water/air interface. Atmospheric and biological chemistry often takes place at interfaces. Our work resulted in a simple, yet accurate tool for simulations of nitrogen oxyanions and oxyacids at microheterogeneous interface environments.

■ ASSOCIATED CONTENT

Supporting Information

The Supporting Information is available free of charge at <https://pubs.acs.org/doi/10.1021/acs.jpcb.9b08172>.

TI method, conformer contribution to hydration free energy, force field parameters for nitrogen oxyanions and oxyacids, effect of charge on nitrogen oxyanion hydration, effect of force field on ionic interactions, convergence of TI, convergence of conformer distribution, position-dependent pK_a shift (PDF)

Force field and molecular topology files for NO_3^- , NO_2^- , HNO_3 , and HNO_2 (ZIP)

■ AUTHOR INFORMATION

Corresponding Author

Rodrigo M. Cordeiro – Centro de Ciências Naturais e Humanas, Universidade Federal do ABC, 09210-580 Santo André (SP), Brazil; orcid.org/0000-0001-7763-4886; Phone: +55 11 49960173; Email: rodrigo.cordeiro@ufabc.edu.br

Authors

Maksudbek Yusupov – Research Group PLASMANT, Department of Chemistry, University of Antwerp, B-2610 Antwerp, Belgium; orcid.org/0000-0003-4591-858X

Jamoliddin Razzokov – Research Group PLASMANT, Department of Chemistry, University of Antwerp, B-2610 Antwerp, Belgium

Annemie Bogaerts – Research Group PLASMANT, Department of Chemistry, University of Antwerp, B-2610 Antwerp, Belgium; orcid.org/0000-0001-9875-6460

Complete contact information is available at: <https://pubs.acs.org/doi/10.1021/acs.jpcb.9b08172>

Notes

The authors declare no competing financial interest.

■ ACKNOWLEDGMENTS

We thank Universidade Federal do ABC for providing the computational resources needed for completion of this work. This study was financed in part by the Coordenação de Aperfeiçoamento de Pessoal de Nível Superior - Brasil (CAPES) - Finance Code 001.

■ REFERENCES

- (1) Pöschl, U. Atmospheric Aerosols: Composition, Transformation, Climate and Health Effects. *Angew. Chem., Int. Ed.* **2005**, *44*, 7520–7540.
- (2) Mensinga, T. T.; Speijers, G. J. A.; Meulenbelt, J. Health Implications of Exposure to Environmental Nitrogenous Compounds. *Toxicol. Rev.* **2003**, *22*, 41–51.
- (3) Brown, S. B.; Brown, E. A.; Walker, I. The Present and Future Role of Photodynamic Therapy in Cancer Treatment. *Lancet Oncol.* **2004**, *5*, 497–508.
- (4) Keidar, M. Plasma for Cancer Treatment. *Plasma Sources Sci. Technol.* **2015**, *24*, 033001.
- (5) Kameda, Y.; Saitoh, H.; Uemura, O. The Hydration Structure of NO_3^- in Concentrated Aqueous Sodium Nitrate Solutions. *Bull. Chem. Soc. Jpn.* **1993**, *66*, 1919–1923.
- (6) Wang, H.-W.; Vlcek, L.; Neuefeind, J. C.; Page, K.; Irle, S.; Simonson, J. M.; Stack, A. G. Decoding Oxyanion Aqueous Solvation Structure: A Potassium Nitrate Example at Saturation. *J. Phys. Chem. B* **2018**, *122*, 7584–7589.
- (7) Tongraar, A.; Tangkawanwanit, P.; Rode, B. M. A Combined QM/MM Molecular Dynamics Simulations Study of Nitrate Anion (NO_3^-) in Aqueous Solution. *J. Phys. Chem. A* **2006**, *110*, 12918–12926.
- (8) Yadav, S.; Choudhary, A.; Chandra, A. A First-Principles Molecular Dynamics Study of the Solvation Shell Structure, Vibrational Spectra, Polarity, and Dynamics around a Nitrate Ion in Aqueous Solution. *J. Phys. Chem. B* **2017**, *121*, 9032–9044.
- (9) Vchirawongkwin, V.; Kritayakornupong, C.; Tongraar, A.; Rode, B. M. Symmetry Breaking and Hydration Structure of Carbonate and Nitrate in Aqueous Solutions: A Study by Ab Initio Quantum Mechanical Charge Field Molecular Dynamics. *J. Phys. Chem. B* **2011**, *115*, 12527–12536.
- (10) Thøgersen, J.; Réhault, J.; Odelius, M.; Ogden, T.; Jena, N. K.; Jensen, S. J. K.; Keiding, S. R.; Helbing, J. Hydration Dynamics of Aqueous Nitrate. *J. Phys. Chem. B* **2013**, *117*, 3376–3388.
- (11) Xie, W. J.; Zhang, Z.; Gao, Y. Q. Ion Pairing in Alkali Nitrate Electrolyte Solutions. *J. Phys. Chem. B* **2016**, *120*, 2343–2351.
- (12) Salvador, P.; Curtis, J. E.; Tobias, D. J.; Jungwirth, P. Polarizability of the Nitrate Anion and Its Solvation at the Air/Water Interface. *Phys. Chem. Chem. Phys.* **2003**, *5*, 3752–3757.
- (13) Lange's Handbook of Chemistry, 15th ed.; Dean, J. A., Ed.; McGraw-Hill, 1999.
- (14) Lewis, T.; Winter, B.; Stern, A. C.; Baer, M. D.; Mundy, C. J.; Tobias, D. J.; Hemminger, J. C. Does Nitric Acid Dissociate at the Aqueous Solution Surface? *J. Phys. Chem. C* **2011**, *115*, 21183–21190.
- (15) Shamay, E. S.; Buch, V.; Parrinello, M.; Richmond, G. L. At the Water's Edge: Nitric Acid as a Weak Acid. *J. Am. Chem. Soc.* **2007**, *129*, 12910–12911.
- (16) Ardura, D.; Donaldson, D. J. Where Does Acid Hydrolysis Take Place? *Phys. Chem. Chem. Phys.* **2009**, *11*, 857–863.
- (17) Wang, S.; Bianco, R.; Hynes, J. T. Depth-Dependent Dissociation of Nitric Acid at an Aqueous Surface: Car–Parrinello Molecular Dynamics. *J. Phys. Chem. A* **2009**, *113*, 1295–1307.
- (18) Baer, M. D.; Tobias, D. J.; Mundy, C. J. Investigation of Interfacial and Bulk Dissociation of HBr, HCl, and HNO_3 Using Density Functional Theory-Based Molecular Dynamics Simulations. *J. Phys. Chem. C* **2014**, *118*, 29412–29420.
- (19) Oostenbrink, C.; Villa, A.; Mark, A. E.; Van Gunsteren, W. F. A Biomolecular Force Field Based on the Free Enthalpy of Hydration and Solvation: The GROMOS Force-Field Parameter Sets 53A5 and 53A6. *J. Comput. Chem.* **2004**, *25*, 1656–1676.
- (20) Otten, D. E.; Onorato, R.; Michaels, R.; Goodknight, J.; Saykally, R. J. Strong Surface Adsorption of Aqueous Sodium Nitrite as an Ion Pair. *Chem. Phys. Lett.* **2012**, *519*–520, 45–48.
- (21) Frenkel, D.; Smit, B. *Understanding Molecular Simulation: From Algorithms to Applications*; Academic Press: San Diego, 2001.
- (22) van Der Spoel, D.; Lindahl, E.; Hess, B.; Groenhof, G.; Mark, A. E.; Berendsen, H. J. C. GROMACS: Fast, Flexible, and Free. *J. Comput. Chem.* **2005**, *26*, 1701–1718.

- (23) Hess, B.; Kutzner, C.; van Der Spoel, D.; Lindahl, E. GROMACS 4: Algorithms for Highly Efficient, Load-balanced, and Scalable Molecular Simulation. *J. Chem. Theory Comput.* **2008**, *4*, 435–447.
- (24) Jayaraman, S.; Thompson, A. P.; Hisatsune, I. C.; Maginn, E. J. Molecular Simulation of the Thermal and Transport Properties of Three Alkali Nitrate Salts. *Ind. Eng. Chem. Res.* **2010**, *49*, 559–571.
- (25) Ohkubo, T.; Ohnishi, R.; Sarou-Kanian, V.; Bessada, C.; Iwadate, Y. Molecular Dynamics Simulations of the Thermal and Transport Properties of Molten NaNO₂–NaNO₃ Systems. *Electrochemistry* **2018**, *86*, 104–108.
- (26) McGraw, G. E.; Räsänen, D. L.; Hisatsune, I. C. Vibrational Spectra of Isotopic Nitric Acids. *J. Chem. Phys.* **1965**, *42*, 237–244.
- (27) Perrin, A. Recent Progress in the Analysis of HNO₃ Spectra. *Spectrochim. Acta, Part A* **1998**, *54*, 375–393.
- (28) Murto, J.; Räsänen, M.; Aspiala, A.; Lotta, T. Ab Initio Calculations on HONO: Energies, Geometries and Force Fields on Different Levels of Theory. *J. Mol. Struct.: THEOCHEM* **1985**, *122*, 213–224.
- (29) McGraw, G. E.; Bernitt, D. L.; Hisatsune, I. C. Infrared Spectra of Isotopic Nitrous Acids. *J. Chem. Phys.* **1966**, *45*, 1392–1399.
- (30) Varma, R.; Curl, R. F. Study of the Dinitrogen Trioxide–Water–Nitrous Acid Equilibrium by Intensity Measurements in Microwave Spectroscopy. *J. Phys. Chem.* **1976**, *80*, 402–409.
- (31) Shirk, A. E.; Shirk, J. S. Isomerization of HONO in Solid Nitrogen by Selective Vibrational Excitation. *Chem. Phys. Lett.* **1983**, *97*, 549–552.
- (32) Cordeiro, R. M. Reactive Oxygen Species at Phospholipid Bilayers: Distribution, Mobility and Permeation. *Biochim. Biophys. Acta, Biomembr.* **2014**, *1838*, 438–444.
- (33) Cordeiro, R. M. Reactive Oxygen and Nitrogen Species at Phospholipid Bilayers: Peroxynitrous Acid and Its Homolysis Products. *J. Phys. Chem. B* **2018**, *122*, 8211–8219.
- (34) Frisch, M. J. et al. *Gaussian 09*; Gaussian Inc.: Wallingford, CT, 2009.
- (35) Jämbeck, J. P. M.; Lyubartsev, A. P. Exploring the Free Energy Landscape of Solutes Embedded in Lipid Bilayers. *J. Phys. Chem. Lett.* **2013**, *4*, 1781–1787.
- (36) Vchirawongkwin, S.; Kritayakornupong, C.; Tongraar, A.; Vchirawongkwin, V. Hydration Properties Determining the Reactivity of Nitrite in Aqueous Solution. *Dalton Trans.* **2014**, *43*, 12164–12174.
- (37) Kameda, Y.; Arakawa, H.; Hangai, K.; Uemura, O. The Structure around the Nitrite Ion in Concentrated Aqueous Solutions. *Bull. Chem. Soc. Jpn.* **1992**, *65*, 2154–2156.
- (38) Ohtaki, H.; Radnai, T. Structure and Dynamics of Hydrated Ions. *Chem. Rev.* **1993**, *93*, 1157–1204.
- (39) Reynolds, J. G.; Mauss, B. M.; Daniel, R. C. The Relative Viscosity of NaNO₃ and NaNO₂ Aqueous Solutions. *J. Mol. Liq.* **2018**, *264*, 110–114.
- (40) CRC *Handbook of Chemistry and Physics*, 84th ed.; Lide, D. R., Ed.; CRC Press, 2004.
- (41) Smith, J. W.; Lam, R. K.; Shih, O.; Rizzuto, A. M.; Prendergast, D.; Saykally, R. J. Properties of Aqueous Nitrate and Nitrite from X-Ray Absorption Spectroscopy. *J. Chem. Phys.* **2015**, *143*, 084503.
- (42) Riddell, J. D.; Lockwood, D. J.; Irish, D. E. Ion Pair Formation in NaNO₃/D₂O Solutions: Raman and Infrared Spectra, Partial Molal Volumes, Conductance, and Viscosity. *Can. J. Chem.* **1972**, *50*, 2951–2962.
- (43) Schmid, N.; Eichenberger, A. P.; Choutko, A.; Riniker, S.; Winger, M.; Mark, A. E.; van Gunsteren, W. F. Definition and Testing of the GROMOS Force-Field Versions 54A7 and 54B7. *Eur. Biophys. J.* **2011**, *40*, 843–856.
- (44) Cordeiro, R. M. Molecular Dynamics Simulations of the Transport of Reactive Oxygen Species by Mammalian and Plant Aquaporins. *Biochim. Biophys. Acta, Gen. Subj.* **2015**, *1850*, 1786–1794.
- (45) Razzokov, J.; Yusupov, M.; Cordeiro, R. M.; Bogaerts, A. Atomic Scale Understanding of the Permeation of Plasma Species across Native and Oxidized Membranes. *J. Phys. D: Appl. Phys.* **2018**, *51*, 365203.
- (46) *Perry's Chemical Engineers' Handbook*, 7th ed.; Perry, R. H., Green, D. W., Maloney, J. O., Eds.; McGraw-Hill, 1999.
- (47) Schwartz, S. E.; Vácha, W. H. Solubility Equilibria of the Nitrogen Oxides and Oxyacids in Dilute Aqueous Solution. In *Advances in Environmental Science and Engineering*; Pfafflin, J. R., Ziegler, E. N., Eds.; Gordon and Breach Science Publishers: New York, 1981; Vol. 4, pp 1–45.
- (48) Sander, R. Compilation of Henry's Law Constants (version 4.0) for Water as Solvent. *Atmos. Chem. Phys.* **2015**, *15*, 4399–4981.
- (49) Minofar, B.; Vácha, R.; Wahab, A.; Mahiuddin, S.; Kunz, W.; Jungwirth, P. Propensity for the Air/Water Interface and Ion Pairing in Magnesium Acetate vs Magnesium Nitrate Solutions: Molecular Dynamics Simulations and Surface Tension Measurements. *J. Phys. Chem. B* **2006**, *110*, 15939–15944.
- (50) Thomas, J. L.; Roeselová, M.; Dang, L. X.; Tobias, D. J. Molecular Dynamics Simulations of the Solution–Air Interface of Aqueous Sodium Nitrate. *J. Phys. Chem. A* **2007**, *111*, 3091–3098.
- (51) Hub, J. S.; Wolf, M. G.; Calemán, C.; van Maaren, P. J.; Groenhof, G.; van der Spoel, D. Thermodynamics of Hydronium and Hydroxide Surface Solvation. *Chem. Sci.* **2014**, *5*, 1745–1749.
- (52) Wren, S. N.; Donaldson, D. J. Glancing-Angle Raman Study of Nitrate and Nitric Acid at the Air–aqueous Interface. *Chem. Phys. Lett.* **2012**, *522*, 1–10.
- (53) Duan, J.; Gan, L.; Nie, L.; Sun, F.; Lu, X.; He, G. On the Penetration of Reactive Oxygen and Nitrogen Species Generated by a Plasma Jet into and through Mice Skin with/without Stratum Corneum. *Phys. Plasmas* **2019**, *26*, 043504.
- (54) Lundberg, J. O.; Weitzberg, E.; Gladwin, M. T. The Nitrate–nitrite–nitric Oxide Pathway in Physiology and Therapeutics. *Nat. Rev. Drug Discovery* **2008**, *7*, 156–167.